Computational fluid dynamics-based surrogate optimization of a wind turbine blade tip extension for maximising energy production

Zahle, Frederik; Sørensen, Niels N.; McWilliam, Michael; Barlas, Athanasios

Published in:
Journal of Physics: Conference Series

Link to article, DOI:
10.1088/1742-6596/1037/4/042013

Publication date:
2018

Document Version
Publisher's PDF, also known as Version of record

Computational fluid dynamics-based surrogate optimization of a wind turbine blade tip extension for maximising energy production

IOP Conf. Series: Journal of Physics: Conf. Series **1037** (2018) 042013 doi:10.1088/1742-6596/1037/4/042013

Computational fluid dynamics-based surrogate optimization of a wind turbine blade tip extension for maximising energy production

Frederik Zahle, Niels N. Sørensen, Michael K. McWilliam, Athanasios Barlas

DTU Wind Energy, Risø Campus, Frederiksborgvej 399, Roskilde, Denmark

E-mail: frza@dtu.dk

Abstract. This article presents a design study into the redesign of a wind turbine blade tip seeking to increase the energy production subject to the loads constraints of the existing blade. The blade shape is parameterized to allow for planform changes in the tip region with respect to chord, twist and blade length extension, and additionally three parameters that allow to explore winglet-like shapes. The design strategy uses 3D computational fluid dynamics computations of the geometrically resolved rotor to create a surrogate model, after which the tip shape is numerically optimized based on the surrogate model, subject to a number of geometric and loads-based constraints. The study shows that it is possible to increase power production by 2.6% for a blade extension with a winglet, without increasing the flapwise bending moment at 90% radius, whereas for a straight blade extension it was only possible to achieve an increase of 0.76%.

1. Introduction

Wind turbine manufacturers have an increasing need to be able to customize wind turbine rotors for specific wind climates and sites, in order to maximise annual energy production (AEP) and thereby reduce cost of energy (CoE). It is often not economically feasible to create completely redesigned blades for only small increases in blade length, and therefore a less intrusive approach needs to be available. One means to achieving this is to design various tip extensions for a given blade, that only replaces the very tip of the original blade, or simply extends it with a sleeve-like solution. A small extension of the blade can lead to several percent increase in AEP, and is therefore a very attractive solution. The challenge is that extending the tip can lead to increases in loads, and a careful design of the tip is therefore crucial for meeting these constraints.

Wind turbine blades are commonly designed using blade element momentum (BEM) based methods, incorporated into an aeroelastic tool. However, BEM based tools suffer from a very simplified empirical approach to the modelling of the flow near the tip, which cannot account for out-of-plane shapes like sweep or winglets unless combined with vortex theory based models. This fact makes these tools inadequate for use in designing the very tip of the blade, since it is well-known that the flow in this region is highly three-dimensional. There are a number works in literature focusing on blade tip design and some, specifically on winglets. Ferrer et al. [1] studied three different tip shapes for the NREL Phase VI rotor, and found that a highly tapered tip ending at the blade quarter-chord location had the best torque to thrust ratio. Gaunaa et

al. [2] studied winglets using a free-wake lifting line code and validated the results using CFD. They found that a winglet pointing downstream was more efficient than one pointing upstream, and that winglets are less efficient with respect to power coefficient increase than an equivalent extension of the blade. In more recent work by Hansen [3] a surrogate model is constructed based on a CFD code modelling a wind tunnel model sized rotor fitted with a winglet. Hansen constructs a Kriging surrogate which is enhanced using an expected improvement criterion to add in-fill points. Although not specifically targetting blade tip design, Sessarego et al. [4] use surrogate modelling to optimize a wind turbine blade based on a panel method, and demonstrate that this methodology is efficient and equally accurate to a BEM based design, showing promise for applying the methodology to more advanced blade designs. Finally, van Kalken et al. [5] conducted a design and field testing study, where three tip extensions were designed, a conventional tip extension, one with a winglet and one with turbulators. Two were tested on a Nordex N80 2.5MW turbine, and it was shown that measured power increases of 2% to 9% could be achieved. The predicted loads were of similar magnitude as the power increase, although this was not reported from the experimental campaign.

In this work we use 3D computational fluid dynamics (CFD) to re-design the blade tip of the IEA-10.0-198 10 MW Reference Wind Turbine, where we seek to explore the blade tip design space with systematic variation of pre-defined degrees of freedom of the tip shape as well as different constraints on sectional loads along the blade. We seek to answer the following questions:

- What is the effect of each of the blade tip geometric parameters on mechanical power?
- Is a winglet-like blade tip shape better than a simple extension of the blade when taking loads constraints into account?
- What is the potential mechanical power gain of extending the IEA-10.0-198 10 MW RWT blade tip subject to loads constraints?

Rather than using numerical optimization directly on the CFD workflow, we use design of experiments (DoE) to train a surrogate model of the CFD code, and apply gradient-based optimization on this computationally much cheaper model. This approach is very attractive because rather than being a one-shot expensive approach, we can explore the design space efficiently with a large number of optimizations with varying degrees of freedom and constraints.

The paper is organised as follows: Firstly, the methodology and tools used are described; secondly, the surrogate model is validated; and thirdly, a series of optimization studies are performed where the effect of key design variables are explored. Finally, a set of tip designs are made, for which the loads constraints are varied, exploring the differences between a straight blade extension and an extension with a winglet.

2. Methodology

The underlying tools used in this work deal with geometry generation, surface mesh generation, volume mesh generation, and finally the flow solution. To efficiently explore the design space, an automated and robust workflow was crucial, since the design space needed to be sampled randomly to generate a surrogate model of the high-fidelity CFD code. In the present study we used Python to wrap the Fortran-based mesh generation and flow solver codes, and combined these with a geometry and surface mesh generation tool written in Python. The workflow is setup using OpenMDAO [6], which handles the case iteration and data transfer between models. In the following sub-sections, the tools used are introduced.

2.1. Geometry Generation

The lofted blade shape is generated based on a blade planform and a series of base airfoils positioned at given spanwise locations. To manipulate the outer part of the blade planform,

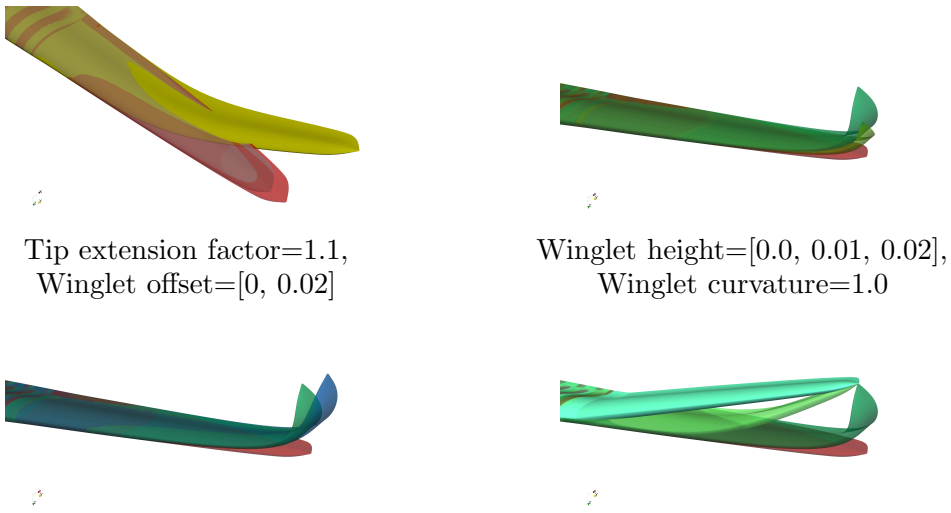

Tip extension factor=1.1,
Winglet offset=[0, 0.02]

Winglet height=[0.0, 0.01, 0.02],
Winglet curvature=1.0

Winglet height=[0.0, 0.02],
Winglet offset=[0.0, 0.015], Winglet curvature=1.0

Winglet curvature=[0., 0.5, 1.0],
Winglet height=[0.0, 0.02]

Figure 1. Effect of changing the four tip geometry parameters.

FFD Bezier splines can be associated with any planform variable. To enable more control of the tip shape a set of dedicated parameters were introduced: the out-of-plane position of the tip, the streamwise offset, the tip curvature factor, and finally a factor controlling the extension of the blade tip. Note that the winglet like shapes all point upstream towards the pressure side of the blade, away from the tower. An in-house tool, *PGL*, was used to parametrically generate the lofted blade shape and CFD surface mesh based on the above described parameters. Figure 1 shows the effects of changing the four tip shape parameters.

2.2. 3D CFD Solver: EllipSys3D

The meshes used in this work were structured grid meshes with an O-O topology. For the surrogate model generation, a somewhat coarse mesh was used: The surface was discretized with 192 cells in the chordwise direction, 96 in the spanwise direction, a tip cap of four blocks of 24×24 cells, with a first cell height of 1×10^{-6}m. The in-house hyperbolic mesh generator HypGrid3D [7] was used to grow the volume mesh into a spherical domain using 96 cells, with the outer boundaries placed approximately 8 rotor diamaters from the rotor. The resulting volume mesh thus contained 5.97 mio. cells. The in-house incompressible Navier-Stokes flow solver EllipSys3D [8, 9, 10] was used assuming steady state flow and fully turbulent boundary layers using the $k-\omega$ SST turbulence model by Menter et al. [11]. To increase efficiency and to speed up the convergence for each point in the sampling process, the tool chain was wrapped in Python using f2py, allowing to directly pass data from the meshing tool to the flow solver, and allowed us to reuse the flow solution from the previous blade shape resulting in a much shorter transient to reach steady state for each case. A single evaluation of a flow solution required approximately 13 minutes of walltime on 216 cores.

3. Baseline rotor

The rotor used in the present study is the IEA-10.0-198 10 MW Reference Wind Turbine[12] designed within the context of the IEA Wind Task 37. The rotor has a diameter of 198 m and is aerostructurally optimized to maximise AEP, subject to constraints on loads to not exceed

those of the DTU 10MW RWT.Figure 2 shows the planform of the blade. In the present study we have for simplicity chosen to remove the prebend from the blade planform.

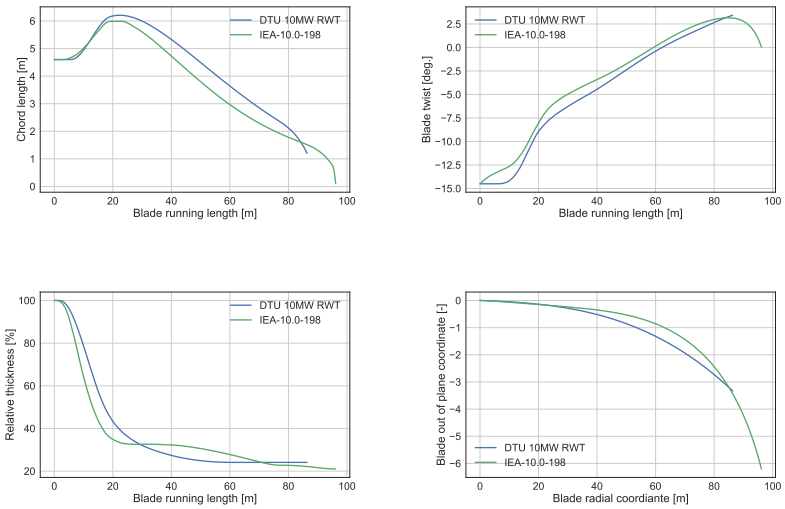

Figure 2. Blade planform compared to the baseline DTU 10MW RWT.

4. Design of Experiments and surrogate modelling

A total of 12 design variables are used in the numerical experiment: four control points for each of the spanwise splines for chord and twist, as well as the tip extension factor, winglet height, winglet offset and winglet curvature, R_{ext}, h_{wl}, s_{wl}, c_{wl}. Optimized Latin Hypercube sampling is used, which randomly samples the design space, but ensures that the sampling points are distributed uniformly throughout the design space. To enable an AEP balanced design, the sampling process is carried out at three discrete wind speeds of [6, 8, 10] m/s. Although more wind speeds would have been desirable to include, in particular for loads constraints, we chose to to use the 10 m/s case for constraining loads, since the rotor at that wind speed is operating very close to maximum flapwise bending moment. A total of 300 sampling points are computed for each wind speed. In this process, only five evaluations failed due to degenerated meshes.

In this work, the classical second order response surface was used to generate the surrogate model. See Reference [13] for an in-depth description of this methodology. To estimate the overall error of the surrogate model, a leave one out cross-validation was done. This involves successively leaving out one sample point, training the model, and comparing the predicted response to the sample point. The error is estimated as the normalised root mean square (NRMSE) as follows:

$$NRMSE = \frac{\sqrt{\sum_{i=1}^{n}(\tilde{y}_i - y_i)^2}}{y_{max} - y_{min}} \tag{1}$$

The overall error of the surrogate was found to be 1.98% for the rotor torque, and 1.29% for the blade flapwise moment at 90% span.

5. Design Studies

In this section a number of optimized designs based on the surrogate model are examined. A first set of designs aim at exploring the three blade tip shape parameters, in an isolated fashion to attempt to shed light on their individual contribution to the power increase of a winglet.

The final two studies investigate the potential power production increase as function of varying flapwise loads constraints, comparing a straight blade extension with a blade extension with a winglet shape.

All the optimized designs in this work are based on the overall problem formulation shown below:

$$\begin{aligned} \text{minimize:} \quad & -\frac{AEP(\mathbf{x})}{AEP(\mathbf{0})} \\ \text{with respect to:} \quad & \text{chord: } c_0, c_1, c_2, c_3 \\ & \text{twist: } \theta_0, \theta_1, \theta_2, \theta_3 \\ & \text{tip shape: } c_{wl}, h_{wl}, s_{wl}, R_{ext} \\ \text{subject to:} \quad & F_x \geq 0.0, \\ & M_{x-con} \leq 0., \\ & \frac{dChord}{dS} \leq 0.0, \end{aligned} \tag{2}$$

where F_x is the tangential force along the blade, on which we impose a constraint, since it was observed that the surrogate model for some cases favoured a small negative driving force on the winglet, which was deemed not valid. M_{x-con} is the flapwise moment constraint imposed at $r/R = 0.9$, defined as:

$$M_{x-con} = F \cdot M_{x-base}|_{r/R=0.9} + (1 - F) \cdot M_{x-free}|_{r/R=0.9} \tag{3}$$

where $M_x|_{r/R=0.9}$ is the sectional flapwise moment at $r/R = 0.9$, linearly weighted with the factor F between the loads on the baseline blade, M_{x-base} and an optimized blade with no loads constraints, M_{x-free}, where F is in the range [0:1]. Note that all loads constraints are based on the surrogate model's prediction of these loads, and not the real model results. A geometric constraint on the chord is enforced to ensure smooth shapes. $\frac{dChord}{dS}$ is the gradient of the chord with respect to the blade running length, which we do not allow to be positive.

5.1. Influence of winglet height

In this study we fixed the tip shape to be a winglet with a 90 degree bend, no sweep, and no blade extension compared to the baseline blade, thus removing R_{ext}, h_{wl}, s_{wl}, c_{wl} as design variables, and only optimizing chord and twist for a range of winglet heights, h_{wl}=[0:0.03], subject to the loads constraints described in Equations 2 and 3 with F=1.0, corresponding to no allowed exceedence of the loads of the baseline blade.

Figure 3 shows the resulting mechanical power normalized with the mechanical power of the baseline blade as function of winglet height. The surrogate model predicts an increase of up to 1.6% for the lower wind speeds, whereas at higher wind speed the benefit is very small. Note also that the surrogate predicts a benefit of a zero height winglet clearly showing that the simple second order polynomial does not capture the model well close to this edge of the design space. Also included in the figure is the performance of the optimized designs evaluated with CFD at 8 m/s, showing a steeper increase in power as function of winglet height. Upon further investigation, it was found that the moment constraint evaluated in the CFD model was exceeded, and increasingly violated for larger winglets.

5.2. Influence of winglet offset

In the next study we fixed the winglet height to 2%, h_{wl}=0.02, set the curvature to one, c_{wl}=1.0, and applied no blade extension, R_{ext}=1.0, and optimized chord and twist for a range of winglet

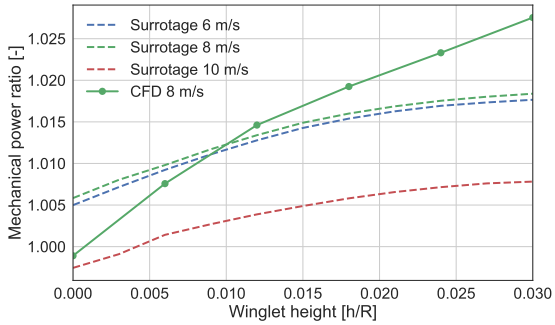

Figure 3. Mechanical power ratio vs winglet height for fixed s_{wl}=0.0, c_{wl}=1.0, and R_{ext}=1.0.

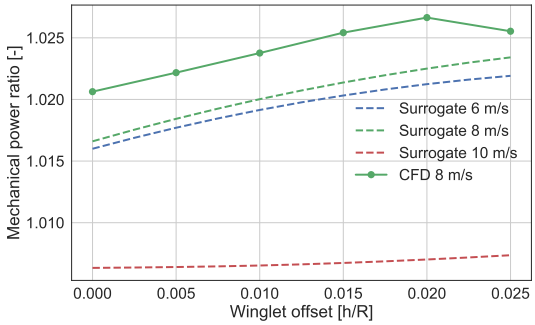

Figure 4. Mechanical power ratio vs winglet sweep for fixed h_{wl}=0.02 and c_{wl}=1.0, and R_{ext}=1.0.

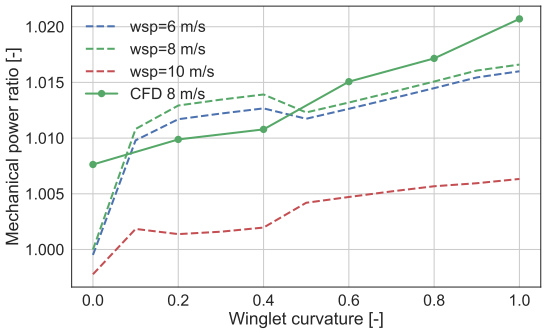

Figure 5. Mechanical power ratio vs winglet curvature for fixed h_{wl}=0.02, s_{wl}=0.0, and R_{ext}=1.0.

sweeps, s_{wl}=[0:0.025], subject to the loads and geometric constraints defined in Equations 2 and 3 with F=1.0.

Figure 4 shows the mechanical power ratio as function of winglet sweep predicted at three wind speeds by the surrogate model, compared to a single wind speed evaluated with CFD. Both the surrogate model and the CFD evaluations predict an increase in power production as function of sweep, although the CFD model appears to have a maximum increase occur at s_{wl}=0.02, which is not captured by the surrogate. The surrogate model predicts an increase in efficiency of 0.67% with added sweep, compared to 0.59% increase when evaluated in CFD.

5.3. Influence of winglet curvature

In the final parameter study we fixed winglet height to 2%, h_{wl}=0.02, set the sweep to zero, s_{wl}=0.0, and optimized chord and twist for a range of winglet curvatures, c_{wl}=[0.:1.], again subject to the loads and geometric constraints defined in Equations 2 and 3 with F=1.0.

Figure 5 shows the mechanical power ratio as function of winglet curvature predicted by the surrogate model compared to the CFD model evaluated for the optimized designs, only for a wind speed of 8 m/s. The results show that it is indeed beneficial to curve the tip to form a

winglet like shape, versus a straight bending of the tip around the r/R=0.95 span location. The increase in mechanical power of a tip curvature c_{wl}=1.0 compared to c_{wl}=0.0, was predicted to be 1.7% by the surrogate model, and 1.3% by the CFD computations. Overall, the results of the CFD evaluations agree fairly well with the surrogate model predictions, except for the blade with zero curvature, where the surrogate model predicts no power increase whereas the CFD evaluation shows a 1% increase in mechanical power.

5.4. Tradeoff between loads and mechanical power

In the final two design studies we optimize the performance of the rotor in one case by only allowing blade extension, optimizing chord and twist, and in the other case also including the winglet shape parameters as design variables, which will help us answer the two main questions posed in this work: Firstly, is there a benefit to using a blade extension with a winglet, as opposed to a simple extension of the blade length? And secondly, what is the potential mechanical power gain of extending the IEA-10.0-198 10 MW RWT blade tip subject to loads constraints?

For each study we sweep the load constraint M_{x-con} from a load factor of 2 compared to the baseline design to a load factor of 1, thus obtaining a pareto front between flapwise moment loads and power production.

Figure 6 shows the resulting pareto fronts of mechanical power vs flapwise bending moment of the two studies for the three wind speeds, [6, 8, 10] m/s, showing in dashed lines the surrogate model predictions, and in solid lines the CFD evaluations. The results show quite clearly that it is possible to achieve a greater increase in mechanical power when using a tip extension with a winglet compared to a conventional tip extension, notably only for the two lower wind speeds, whereas the power increases are similar for the two extension types at 10 m/s. For the two lower wind speeds we see that it is possible to increase the mechanical power by 2.6% without increasing flapwise bending moment loads at r/R=0.9, whereas it is only possible to achieve an increase of 0.76% for a straight blade extension. A successive relaxation of the loads constraint shows a consistent offset between the two types of tip extension. Figure 7 shows that it requires approximately 2% extra blade length to achieve the same power increase with extension-only designs compared to the designs with winglet, which has a 3% winglet, but have an approximately 10% higher load level at r/R=0.9 compared to the extension with winglet to produce the same power increase compared to the baseline design.

As to the accuracy of the surrogate model compared to the CFD evaluations, we can in Figure 6 see that the ratio between mechanical power ratio and flapwise loads is captured very well, except for a small offset. The absolute levels of the flapwise moment loads predicted by the surrogate differ by on average 6.8% compared to the CFD model, whereas the power is predicted with an average error of 0.2%.

6. Discussion

Figure 8 shows the chord and twist distributions of the blade extension designed with a winglet and the extension-only design compared to the baseline blade. Both designs feature a reduced chord compared to the baseline blade, and both twist distributions have increased twist in the region r=[96:99] m, followed by a sharp reduction at the outer-most part of the blade.

Figure 9 shows the local power and thrust coefficients along the blade evaluated with CFD at 8 m/s for the M_{x-con}=1.0 designs compared to the baseline blade. As discussed in the previous section, the resulting moment constraints are not equal to the baseline design for either of the tip extension designs, but a comparison is nonetheless interesting in order to further the understanding of the optimized loading distributions of these designs. Evidently, the optimized winglet design has a very low loading on the winglet, both in the tangential and normal direction to the rotor plane. The winglet does not to any significant extent contribute to the increase in power production achieved. Its main role is to displace and diffuse the tip vortex, thus reducing

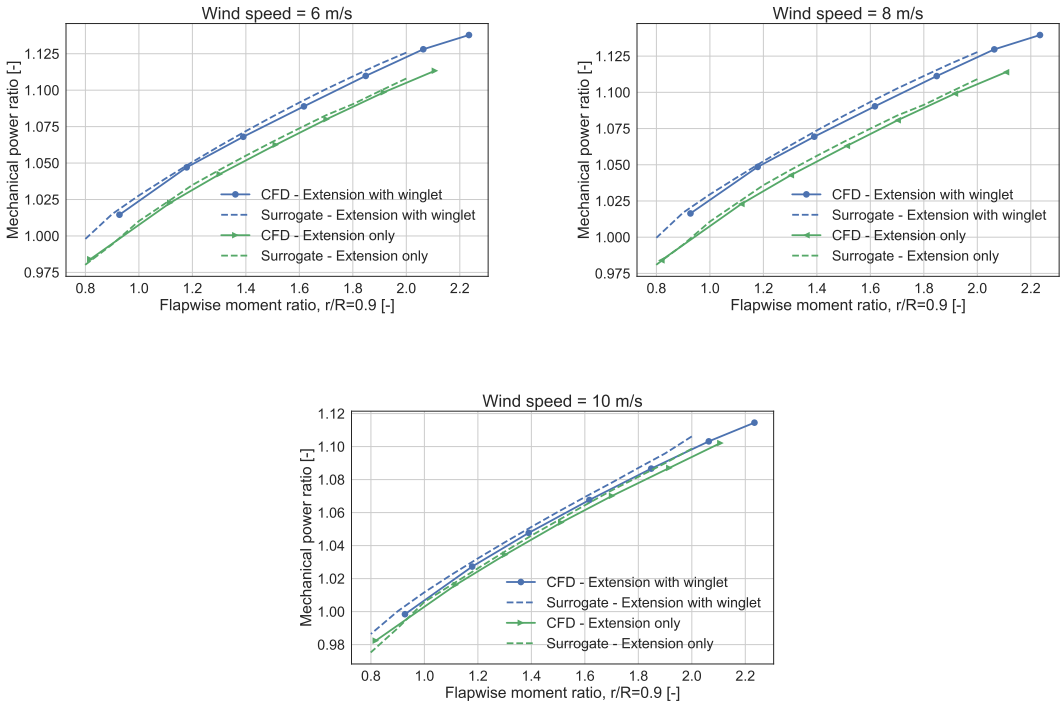

Figure 6. Pareto front of mechanical power production vs flapwise bending moment at r/R=0.9.

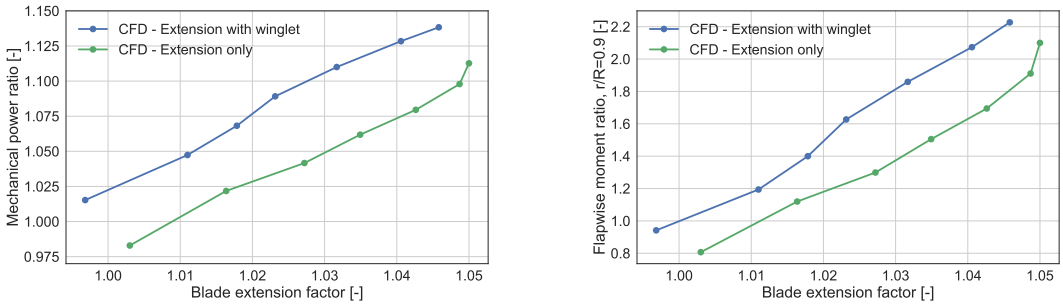

Figure 7. Mechanical power and flapwise moment ratios vs blade extension factor for the tip extension only and extension with winglet, respectively.

the induced drag, while minimising the added flapwise loads. The winglet design has an increase in driving force visible across the outer 50 m of the blade, which stems from the reduction in induced drag. For the straight blade design, on the other hand, the increase in driving force comes primarily from the extension of the blade.

Figure 10 shows a visualisation of the flow behind the optimized tip with a winglet, compared to the baseline design. The optimized design has a tip vortex that is smeared out along the vertical part of the tip, as opposed to the baseline design that has a significantly more concentrated tip vortex. The slight increase in vorticity further inboard is due to a somewhat abrupt reduction in chord, resulting in a change in loading and thus shedding of vorticity.

In this study only steady state loads constraints on the flapwise moment at r/R=0.9 have been

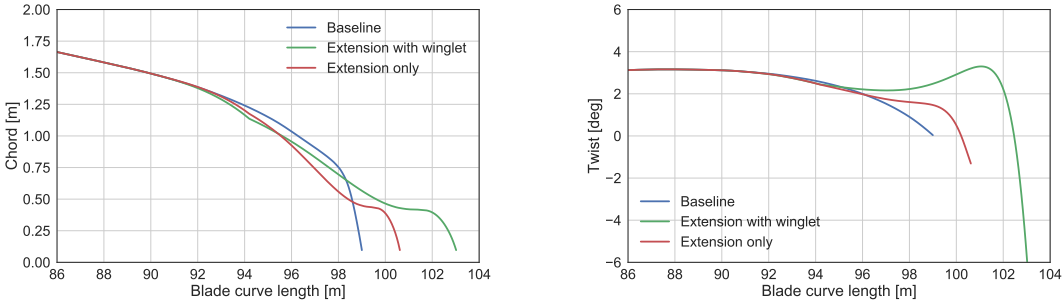

Figure 8. Chord and twist distributions of the two blades designed to not exceed the flapwise moment constraint of the baseline blade.

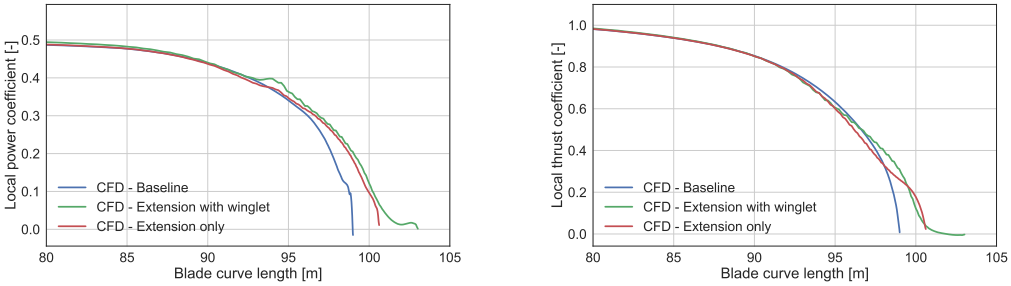

Figure 9. Local power and thrust coefficients along the blade evaluated with CFD at 8 m/s.

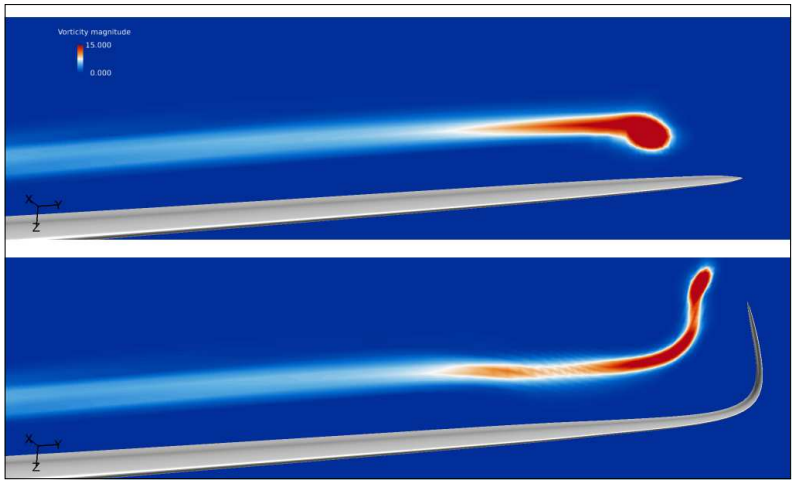

Figure 10. Flow visualisation of vorticity magnitude in a plane 6 m behind the blade in the chordwise direction, showing the baseline blade (top) and the blade with an optimized tip extension with winglet with no increase in flapwise moment at r/R=0.9.

considered. Although not shown here, the root flapwise moments and rotor thrust were both lower than or equal to the baseline design for the design with no excedence of loads at r/R=0.9.

However, considering only steady state loads is a simplification compared to realistic load cases for which wind turbine rotors have to be designed. Further work is needed to firstly evaluate the candidate designs developed in this work for more complex load cases, and secondly, incorporate key load cases into the surrogate modelling framework as constraints in the optimization of the blade tip. Additionally, we seek to include aeroelastic tailoring into the blade tip design, allowing for passive load alleviation such as torsional couplings, to come closer to the notion of a smart blade tip, with even higher potential AEP increase without incurring increases in loads.

7. Conclusion

In this work the potential for increasing the aerodynamic efficiency of a 10 MW rotor subject to flapwise moment loads constraints was investigated. It was found that a blade tip extension with a winglet could achieve a 2.6% increase in power production without increasing flapwise moment loads at r/R=0.9. An equivalent design with a simple tip extension only achieved a 0.76% increase in power production, through a 0.5% increase in blade length. The study also showed that to achieve an equivalent power increase with a tip extension compared to a tip extension with a winglet, 10-15% increase in loads was incurred. Overall, this points to the conclusion that a winglet is indeed beneficial for increasing power production of a wind turbine when subject to loads constraints. Concerning the influence of the three design parameters relating to the winglet shape, we saw that increasing curvature from a simple linear bend of the tip to a winglet-like shape was as expected beneficial. Further, we found that sweeping the winglet downstream also had a beneficial effect. Increasing winglet height up to 3% also had an increasing benefit, although the optimized designs did not meet the loads constraints imposed on the surrogate model.

Acknowledgements

This work is financed under the project "Smart Tip" funded by Innovation Fund Denmark, contract number 7046-00023B.

References

[1] Ferrer E and Munduate X 2007 *Journal of Physics: Conference Series* **75** 012005
[2] Gaunaa M and Johansen J 2007 *Journal of Physics: Conference Series* **75** 012006
[3] Hansen T 2017 *Aerodynamic Optimisation of Airfoils and Winglets for Wind Turbine Application* Ph.D. thesis NTNU
[4] Sessarego M, Ramos García N, Yang H and Shen W 2016 *Renewable Energy* **93** 620–635 ISSN 0960-1481
[5] van Kalken J H and Ceyhan-Yilmaz O 2017 Innotip end report Tech. Rep. ECN: ECN-O–17-011 Energy Research Center of the Netherlands
[6] 2017 http://openmdao.org
[7] Sørensen N N 1998 HypGrid2D—a 2-D mesh generator Tech. rep. Risø-R-1035(EN), Risoe National Laboratory
[8] Michelsen J A 1992 Basis3D—a platform for development of multiblock PDE solvers Tech. Rep. AFM 92-05 Technical University of Denmark
[9] Michelsen J A 1994 Block structured multigrid solution of 2D and 3D elliptic PDEs Tech. Rep. AFM 94-06 Technical University of Denmark
[10] Sørensen N N 1995 General purpose flow solver applied to flow over hills Tech. Rep. Risø-R-827(EN) Risoe National Laboratory
[11] Menter F R 1993 Zonal two-equation $k-\omega$ models for aerodynamic flows *AIAA paper 93-2906*
[12] 2018 https://github.com/ieawindtask37/iea-10.0-198-rwt
[13] Box G E P and Draper N R 1987 *Empirical Model-building and Response Surfaces* (Wiley)